Measurement Science and Technology

100 year anniversary
Measurement Science and Technology

PAPER

Bolt loosening angle detection based on binocular vision

IOP Publishing Measurement Science and Technology
Meas. Sci. Technol. **34** (2023) 035401 (12pp) https://doi.org/10.1088/1361-6501/aca218

Bolt loosening angle detection based on binocular vision

Shixu Wang, Jiang Wu*, Zheng Zhao, Yixin Du, Shuiting Ding and Farong Du

Research Institute of Aero-Engine, Aircraft/Engine Integrated System Safety Beijing Key Laboratory, Beihang University, Beijing 100191, People's Republic of China

E-mail: wu_jiang@buaa.edu.cn

Received 7 September 2022, revised 5 November 2022
Accepted for publication 11 November 2022
Published 5 December 2022

Abstract

Bolt looseness detection is critical in preventing bolt connection failure. Compared to traditional sensor-based bolt looseness detection, image-based methods are low-cost and contactless and have thus become the highlight of research. However, current monocular vision-based detection methods are prone to error scaused by the camera perspective . In this paper, we present a novel bolt loosening angle detection method based on binocular vision. Key points on the bolt are detected and matched by SuperPoint Gauss network for 3D coordinates reconstruction and motion tracking. The bolt loosening angle is solved by fitting the rotation equation using random sample consensus. Experiments verify the proposed method performs well under different perspectives of camera and illumination conditions with an average error of 1.5°. Comparative test shows our method is superior to the monocular vision-based method in terms of accuracy when there is a large perspective angle. The proposed method is mark-free and robust to various working conditions, which makes it of great value for engineering application.

Keywords: bolt loosening angle detection, binocular vision, key point detection, deep learning, 3D reconstruction

(Some figures may appear in colour only in the online journal)

1. Introduction

Bolted connections are widely used in various mechanical structures for its practicality. However, bolts may self-loosen in service because of temperature fluctuation, load cycles and vibration, which impairs the safety and reliability of structures [1]. In terms of aero engine, loose bolted connection could lead to the change of rotor unbalance, which will cause vibration failure of the rotor [2]. In order to prevent the vibration fault of engine caused by bolted connection failure, it is of great importance to detect the bolt looseness in real time [3].

Researchers have developed various approaches to detect bolt loosening using vibration-based and impedance-based techniques [4–6], artificial neural network have also been applied in recent works [7, 8]. However, those traditional methods are usually complex and expensive to implement. Image-based detection methods, by contrast, are contactless, low-cost, and flexible for application. With the development of deep learning and the good performance of convolutional neural network (CNN) used in computer vision, recently researches have focused on vision-based methods of bolt looseness detection. With image information, nut-bolt loss could be detected using deep learning technology such as you only look once (YOLO) algorithm [9]. Some researchers identify the bolt looseness by detecting the exposed length of the screw. Cha *et al* [10] trains a support vector machine using horizontal and vertical lengths of bolt heads based on Hough transform (HT) to automatically distinguish the loosened bolts from the intact bolts, Ramana proposed a similar method based on Viola–Jones algorithm [11]. Zhang *et al* classify intact

* Author to whom any correspondence should be addressed.

bolts and loosened bolts exposed screw using fast region-CNN (R-CNN) [12]. Sun *et al* obtain the three-dimensional information of the edge based on binocular vision, and determine whether the bolt is loosened by calculating the distance between the bolt head and the mounting surface [13].

On the other hand, some researchers detect the bolt looseness by the bolt loosening angle. Figure 1 [14] shows that the rotation angle indicates the loss of preload during the self-loosening process of bolt as the preload declines along with the rotation angle increase. Therefore, it is a feasible approach to predict and prevent bolted connection failure by detecting the bolt loosening angle. Kong and Li realize bolt loosening detection by image registration that woks when the bolt rotation angle is larger than 10° [15]. Nguyen *et al* propose an algorithm to identify bolt loosening angle in steel structure with image processing technology [16], using HT to identify and segment the image of each bolt and detect the rotation angle. Liao Rutian realizes bolt looseness detection based on region-based fully convolutional networks and HT [17]. Huynh *et al* detect the bolt position with R-CNN and Faster R-CNN, correct the distorted image using a perspective correction method based on homography transformation, and used HT to automatically estimate the bolt loosening angle [18–21]. Wang *et al* apply a digit recognition method based on CNN to locate bolts, and use HT and density-based spatial clustering of applications with noise methods to detect bolt rotation angles [22]. Zhao *et al* use single shot detection to identify the bolt loosening angle by locating two types of pattern on the bolt [23]. Yabin *et al* improve the detection accuracy by sticking circular markers on the bolts and point out that the early-stage bolt looseness could be detected by the small rotation angle of bolt [24]. Yang *et al* train a YOLO-based detector to identify loosened bolted connections by making marks on the bolt and nut, however, it cannot quantify the looseness and requires extra manual marking [25].

Figure 1 shows that the loss of preload is up to more than 80% when bolt loosening angle reaches 60°. In order to prevent bolt connection failure, it is critical to identify bolt loosening angle at early stage. This requires bolt loosening detection algorithm should be capable of showing bolt loosening angle in time instead of only identifying loosened bolts [10–12, 15, 25] or missing nut-bolt [9] without quantified results. When the loosening angle goes larger, loosened bolts can be identified by detecting the exposed length of the screw [13]. Among bolt loosening angle detection methods based on monocular vision mentioned above, the HT-based detection method requires a high contrast between the bolt surface color and the background color, otherwise the edge cannot be correctly detected [16–21]. The measurement accuracy is low if the angle is calculated by localizing two patterns of the bolt using the object detection [23], while the method of manually making the mark is not practical under general working conditions [24]. In addition, since the camera is not always perpendicular to the surface of the bolt head, the captured image is the projection of the three-dimensional structure, and the angle information is obtained with errors when using the algorithm of plane geometry. Although it is proposed in related works [18–22] to correct the distorted image using homography matrix, the method is not universally applicable since it only functions when the arrangement of bolts forms a certain shape (such as a circle or a rectangle).

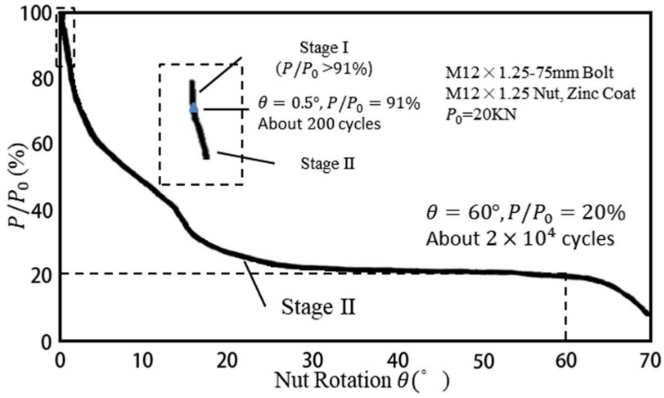

Figure 1. The self-loosening process of bolt (data obtained from [14]).

In view of the problems existing in the current machine vision-based bolt loosening detection methods, we present a new method where binocular vision is introduced to reconstruct the three-dimensional coordinates of key points on the bolt surface, and the bolt loosening angle is calculated by tracking the spatial transformation of the key points. Compared to fastener looseness detection methods based on 3D point cloud from structural light [26–28], the binocular vision-based method is relative low-cost and could produce a quantified loosening angle.

In this paper, our method is illustrated in detail in section 2: theories about the object detector and the key point detector are elaborated in sections 2.1 and 2.2; the algorithm used to solve the loosening angle of the bolt is introduced in section 2.3. Section 3 shows the experimental result that verifies the feasibility and the superiority of the proposed method of bolt loosening angle detection. Meanwhile, our method does not rely on manual marking or specific arrangement of the bolts, therefore it has better applicability.

2. Method and theory

The implementation of the proposed method is shown in figure 2. First, when the bolt is intact, images of the bolt are taken by the binocular cameras simultaneously, and the bolt images are cropped by object detection. Then the key points are detected and matched across the left and right images, and the three-dimensional coordinates of the bolt key points are obtained through three-dimensional reconstruction (stereo matching in figure 2). After the bolt is loosened, the above process is repeated. For each camera, the key points are matched across the two images captured before and after loosening (motion matching in figure 2). The three-dimensional coordinates of the corresponding points are filtered by random sample consensus (RANSAC) algorithm to fit the rotation equation to solve the loosening angle θ.

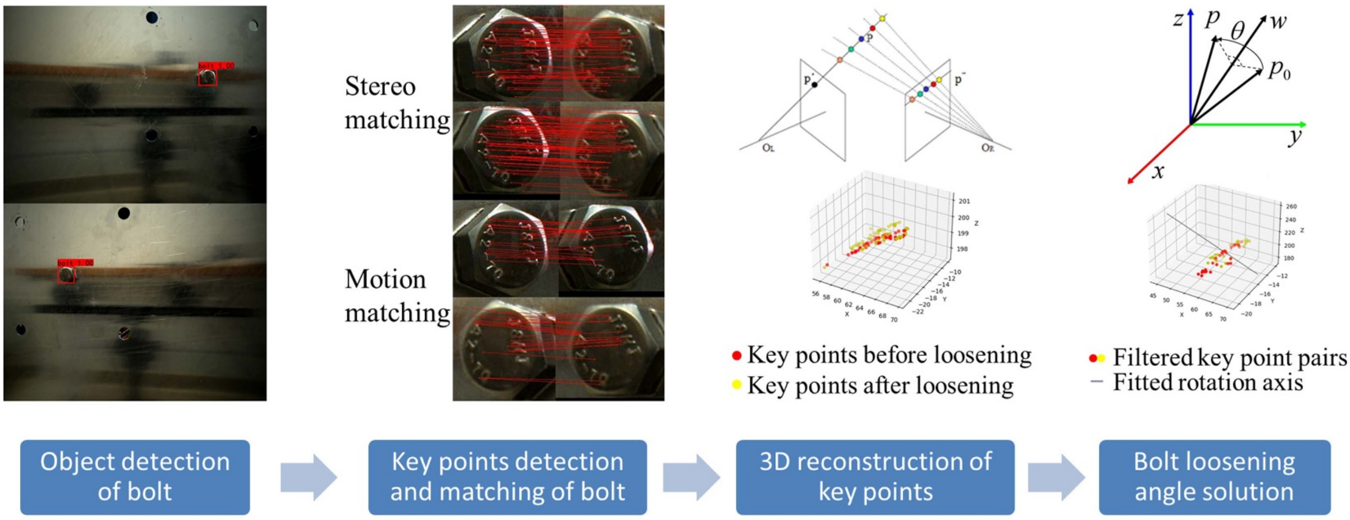

Figure 2. Overview of the proposed bolt looseness detection method.

2.1. Object detection of bolt based on YOLO v4

Bolt only takes up a small region in the image captured by the camera, which adds difficulty to the object detection task. Among the prevalent object detectors based on CNN, YOLO v4 [29] possesses strong feature extraction capability due to the design of residual network and path aggregation network, which makes it competent to the detection task of small objects in terms of both detection speed and accuracy.

We use Hikvision industrial camera to collect 810 pictures for bolt object detection dataset (656 for training, 73 for verification, 81 for test), and label the dataset with LabelImg. The dataset contains bolt images with different backgrounds shot under various conditions as shown in figure 3. YOLO v4 model is trained on NVIDIA p4000 GPU using Pytoch. Based on transfer learning, the weight of backbone is frozen in the first 20 epochs, and the learning rate is set to 0.001; then all weights are unfrozen, the learning rate is set to 0.0001; with Adam optimizer used for gradient descent. After 100 epochs of training, the loss of training set is 0.7524, and the loss of verification set is 0.5789. Precision $=$ 94.90%, Recall $=$ 94.92%, F_1 $=$ 0.95. The test results show it is robust to bolt size, shooting distance and lighting conditions with high accuracy.

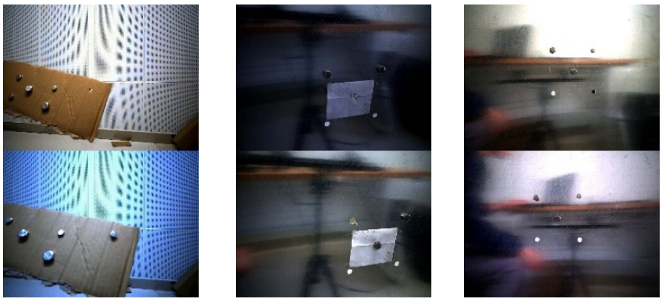

Figure 3. Bolt images shot under various conditions.

2.2. Key points detection of bolt based on SuperPoint Gauss (SPG)

Key points refer to the pixels in the image that are invariant to image scaling and rotation, and partially invariant to change in illumination and 3D camera viewpoint [30]. Matching the key points across two images is the basis of three-dimensional reconstruction and object tracking.

Detone *et al* proposed SuperPoint, a key point detection algorithm based on deep learning [31]. The algorithm is self-supervised where the pseudo labels of key points in the image are produced by a model pretrained on synthetic dataset, then the model is trained with warped image pairs and the pseudo labels. Yau *et al* improved SuperPoint toSPG with sub-pixel accuracy using Gaussian convolution and softmax [32].

In this paper, we train SPG with different backbones (VGG [33], a network proposed by Visual Geometry Group; and CSP Darknet53 [29], the network used in YOLO v4) and different input image types (gray-scale image and RGB image) on Common Object in Context (COCO, a dataset proposed by Microsoft that contains 328k images) [34]. Then the key point detection metrics of each model are evaluated on HPatches [35], as shown in table 1. The RGB detection model with VGG as the backbone has higher matching score due to its matched encoder–decoder network (see figure 4) and richer information contained in RGB images, so we choose VGG-SPG-RGB as the key point detector for further research.

In order to make the key point detection model more accurately identify the key points on the bolt, a bolt image set is made using the trained YOLO v4, with 1565 images for the training set and 173 images for the verification set. The VGG-SPG-RGB model pretrained on the COCO dataset is further

Table 1. Metrics of various key point detection models based on SPG.

	Homography estimation epsilon = 1/3/5			Descriptor metric	
Task	1	3	5	NN mAP	Matching score
VGG-SPG-GRAY (ORIGINAL)	0.46	0.75	0.81	0.78	0.42
CSP Darknet53-SPG-GRAY	0.27	0.63	0.72	0.66	0.39
VGG-SPG-RGB	0.41	0.74	0.81	0.77	0.45
CSP Darknet53-SPG-RGB	0.39	0.72	0.79	0.73	0.44

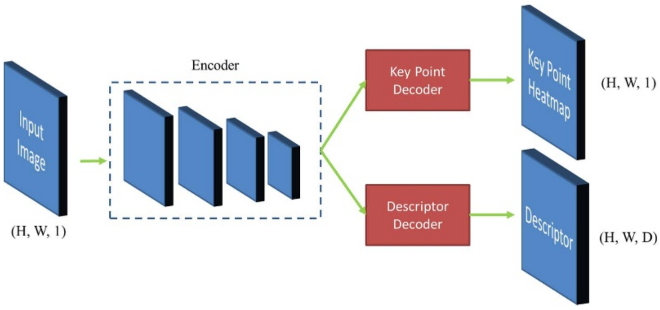

Figure 4. SPG network.

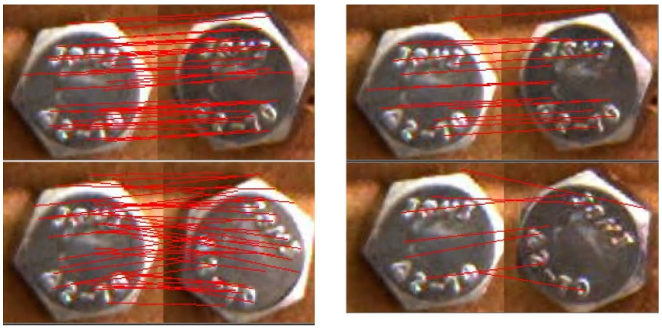

a. SPG-COCO-RGB predictions **b. SPG-Bolt-RGB predictions**

Figure 5. The predictions of key point matches by the SPG network trained on the COCO dataset and the bolt dataset (nn thresh = 1.0).

trained on the bolt dataset to enhance the ability of extract key points in bolt images.

The predictions of key point matches by the SPG network trained on the COCO dataset and the bolt dataset are shown in figure 5. It shows that under the same key point score threshold, the network trained on bolt dataset predicts less matches with lower the proportion of false matches, indicating that the network trained on bolt dataset is able to extract more distinguishable bolt surface texture feature.

2.3. Three-dimensional reconstruction of key points of bolt

According to the imaging principle of pinhole camera, the world coordinates of three-dimensional points $\begin{bmatrix} X_W & Y_W & Z_W \end{bmatrix}^{\mathrm{T}}$ and the pixel coordinates projected on the left and right image plane $\begin{bmatrix} u_L & v_L \end{bmatrix}^T$, $\begin{bmatrix} u_R & v_R \end{bmatrix}^T$ satisfy equation (1):

a. Matches predicted by SPG **b. Matches filtered by the polar constraint**

Figure 6. Stereo matches verification using the polar constraint.

$$Z_{cL}\begin{bmatrix} u_L \\ v_L \\ 1 \end{bmatrix} = \boldsymbol{P_L}\begin{bmatrix} X_W \\ Y_W \\ Z_W \\ 1 \end{bmatrix}, \; Z_{cR}\begin{bmatrix} u_R \\ v_R \\ 1 \end{bmatrix} = \boldsymbol{P_R}\begin{bmatrix} X_W \\ Y_W \\ Z_W \\ 1 \end{bmatrix} \tag{1}$$

where Z_{cL}, Z_{cR} are scaling factors, $\boldsymbol{P_L}$, $\boldsymbol{P_R}$ are the projection matrix of the left and right camera respectively. By using the chess board to calibrate the binocular camera [36], the intrinsic matrix and extrinsic matrices of the camera can be obtained, then $\boldsymbol{P_L}$, $\boldsymbol{P_R}$ can be solved. By matching the key points across two pictures taken by the left and right cameras at certain state (before or after the bolt is loosened), the three-dimensional coordinates of the matched key points can be obtained according to equation (1).

It is found in test that the number of key points that simultaneously meet the binocular matching and the tracking matching is too small to correctly fit the three-dimensional rotation equation. We adopt a strategy where homography transformation is introduced to expand the matched point pairs of left and right cameras. The specific implementation is as follows. First, stereo matches are filtered as shown in figure 6 using the polar constraint [37] that the corresponding pixel coordinates $\begin{bmatrix} u_L & v_L \end{bmatrix}^{\mathrm{T}}$ and $\begin{bmatrix} u_R & v_R \end{bmatrix}^{\mathrm{T}}$ shall satisfy equation (2):

$$\begin{bmatrix} u_L \\ v_L \\ 1 \end{bmatrix} F \begin{bmatrix} u_R \\ v_R \\ 1 \end{bmatrix}^{\mathrm{T}} = 0 \tag{2}$$

where $\boldsymbol{F}$ is the fundamental matrix of binocular camera, which can be obtained by calibration. Taking account of allowed errors, we determine stereo matches that satisfy equation (3) are correct matches, otherwise are mismatches to be filtered. In this paper, the threshold ε is set as 1.0 assuming the allowable error is 1.0 mm in the world coordinate system:

$$\begin{bmatrix} u_L \\ v_L \\ 1 \end{bmatrix} F \begin{bmatrix} u_R \\ v_R \\ 1 \end{bmatrix}^{\mathrm{T}} < \varepsilon \tag{3}$$

Meanwhile, stereo corresponding points satisfy equation (4) where s is the scaling factor and $\boldsymbol{H}$ is the homography matrix:

$$s \begin{bmatrix} u_R \\ v_R \\ 1 \end{bmatrix} = H \begin{bmatrix} u_L \\ v_L \\ 1 \end{bmatrix} = \begin{bmatrix} H_{11} & H_{12} & H_{13} \\ H_{21} & H_{22} & H_{23} \\ H_{31} & H_{32} & 1 \end{bmatrix} \begin{bmatrix} u_L \\ v_L \\ 1 \end{bmatrix}. \tag{4}$$

The RANSAC algorithm [38] is adopted to exclude the mismatches that do not satisfy equation (4), and the homography matrix $\boldsymbol{H}$ is obtained by fitting the inliers. Through $\boldsymbol{H}$ and $\boldsymbol{H}^{-1}$ more matching point pairs are produced: images captured by certain camera before and after loosening are matched for tracking. For the matched point $p_L = \begin{bmatrix} u_L & v_L \end{bmatrix}^{\mathrm{T}}$ at certain state (before or after loosening) of the left image, the corresponding point $p_R' = \begin{bmatrix} u_R' & v_R' \end{bmatrix}^{\mathrm{T}}$ in the right image is obtained by equation (5); for the point $p_R = \begin{bmatrix} u_R & v_R \end{bmatrix}^{\mathrm{T}}$ of the right image, the corresponding point $p_L' = \begin{bmatrix} u_L' & v_L' \end{bmatrix}^{\mathrm{T}}$ in the left camera is obtained by equation (6):

$$u_R' = \frac{H_{11}u_L + H_{12}v_L + H_{13}}{H_{31}u_L + H_{32}v_L + H_{33}}, v_R' = \frac{H_{21}u_L + H_{22}v_L + H_{23}}{H_{31}u_L + H_{32}v_L + H_{33}} \tag{5}$$

$$u_L' = \frac{H_{11}^{-1}u_L + H_{12}^{-1}v_L + H_{13}^{-1}}{H_{31}^{-1}u_L + H_{32}^{-1}v_L + H_{33}^{-1}}, v_L' = \frac{H_{21}^{-1}u_L + H_{22}^{-1}v_L + H_{23}^{-1}}{H_{31}^{-1}u_L + H_{32}^{-1}v_L + H_{33}^{-1}}. \tag{6}$$

With 2D point pair (p_L, p_R') and (p_L', p_R) acquired, the 3D coordinate corresponding to each 2D point pair can be solved by equation (1) and the 3D reconstruction of key points on the bolt is realized.

2.4. Solution to the bolt loosening angle based on binocular vision

Through key point matching, the original coordinate $P = (x, y, z)^{\mathrm{T}}$ before loosening and the transformed coordinate $P' = (x', y', z')^{\mathrm{T}}$ after loosening of the same point on the bolt surface can be obtained. The loosening of the bolt can be simplified as the rotation of the bolt around its own axis, so the bolt loosening angle θ can be solved according to equation (7) which describes three-dimensional rotation of rigid body:

$$\begin{cases} \boldsymbol{P}' = \boldsymbol{R}\boldsymbol{P} \\ \boldsymbol{R} = a\boldsymbol{I} + (1-a)nn^{\mathrm{T}} + b\begin{bmatrix} 0 & -n_z & n_y \\ n_z & 0 & -n_x \\ -n_y & n_x & 0 \end{bmatrix} \\ a = \cos\theta \\ b = \sin\theta. \end{cases} \tag{7}$$

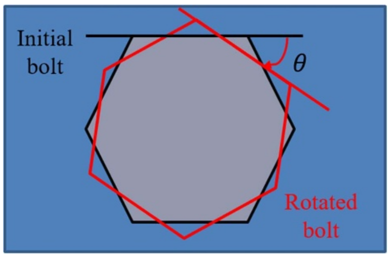

Figure 7. Bolt loosening angle θ.

Algorithm 1. Rotation angle solution using RANSAC.

Input:
Matched point-pair set $S = \{S_1(P_1, P_1'), S_1(P_1, P_1'), \ldots, S_N(P_N, P_N')\}$
Random sample size n
Max iterations max_iter
Expected probability to obtain a correct model p
Residual threshold σ
Process:
initialize most_inliers $= 0$, best_index $= \{\}$, i $= 0$
while i $< \min(\mathrm{max_iter}, \mathrm{end_iter})$ do:
  current_inliers $= 0$, current_index $= \{\}$
  randomly sample n pairs in S to fit (7) and get a model
  for $j = 0, 1, \ldots, N$ do:
    if $e_j = \boldsymbol{P_j}' - \boldsymbol{R}\boldsymbol{P_j} < \sigma$:
      current_inliers $=$ current_inliers $+ 1$
      current_index.append(j)
  end for
  if current_inliers $>$ most_inliers:
    most_inliers $=$ current_inliers
    best_index $=$ current_index
    end_iter $= \frac{\log(1-p)}{\log\left(1-\left(\frac{\mathrm{most\_inliers}}{N}\right)^n\right)}$
  if most_inliers $> 0.5N$: break
end while
return the angle θ solved by fitting (7) using $S_k \in S$, $k \in$ best_index

where $\boldsymbol{R}$ denotes the rotation matrix, θ is the rotation angle (see figure 7), $\boldsymbol{n} = (n_x, n_y, n_z)$ is the unit vector of the rotation axis. Through the coordinates before and after the rotation of multiple key points, the inliers are selected with mismatches excluded by RANSAC algorithm as shown in algorithm 1. The bolt loosening angle θ can be solved by least square fitting using the inliers, where the residual error $e = \boldsymbol{P}' - \boldsymbol{R}\boldsymbol{P}$ is minimized.

In practical use, since the cameras are not mounted on the same board as the bolt is, there may be a relative rotation between the cameras and the board on account of the unstable structure. This, however, has not been considered in previous works [16–24]. In this case (see figure 8), the bolt loosening angle θ should be the relative rotation angle between the bolt and the background (cameras as the viewpoint), namely, $\theta = \theta_1 - \theta_2$. An experiment is conducted to verify the feasibility of bolt loosening angle detection in this case (see section 3.3).

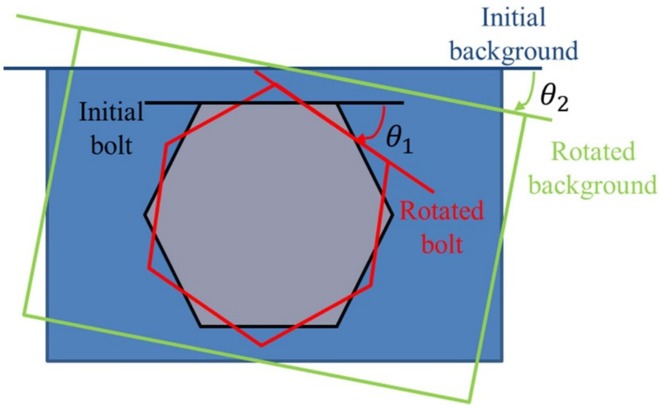

Figure 8. Bolt rotation and background rotation.

3. Experiments and results

3.1. Design and calibration of the workbench for experiment

In order to verify the feasibility of the proposed algorithm, the accuracy measurement experiment of bolt looseness detection based on binocular vision is carried out. The layout of the experimental workbench is shown in figure 9. Two Hikvision cameras (detailed in table 2) are mounted on a tripod, and the data is transmitted to the computer through the Gige data line. The M8 bolts are fixed on the aluminum profile structure, the looseness of which is to be detected. When testing, the vertical angle of the cameras α is alterable by adjusting the tripod (see figure 10(a)), while the relative position with the horizontal angle β between the cameras are fixed (see figure 10(b), $\beta = 20°$). The horizontal distance between the cameras and the background is 25 cm.

In the previous researches of detecting bolt loosening angle based on machine vision, the actual bolt rotation angle in the experiment is usually measured by protractor or directly measured on the picture using image processing tools, which introduces large measurement errors [16–24]. Therefore, we propose to use a servo motor to rotate the bolt, which provides high-precision actual value of bolt rotation angle through closed-loop position control. The 4108 motor and SimpleMotor drive board used in the experiment are shown in figure 11. The AS5600 encoder attached to the motor has 12-bit accuracy with minimum measured angle at 0.1°. The motor is fixed on the aluminum profile workbench. An experiment is conducted as shown in figure 12 in order to calibrate the accuracy of the bolt rotation angle output by the motor: first, the motor is controlled to rotate to 0°, and the position of the pointer edge l_0 is recorded on the background paper. Then the motor is set to rotate 10°, 20°, 30°, 40°, 50° and 60° in sequence, and the pointer positions $l_1, l_2, l_3, l_4, l_5, l_6$ are recorded respectively. At last, the background paper is taken off and the angle between l_i ($i = 1,2,3,4,5,6$) and l_0 is measured by an angle ruler.

The measurement curve obtained from the experiment is shown in figure 13. The average error between the angle measured by the encoder and the angle ruler is within 0.5°, which proves our measurement using motor encoder provides a rather accurate actual rotation angle.

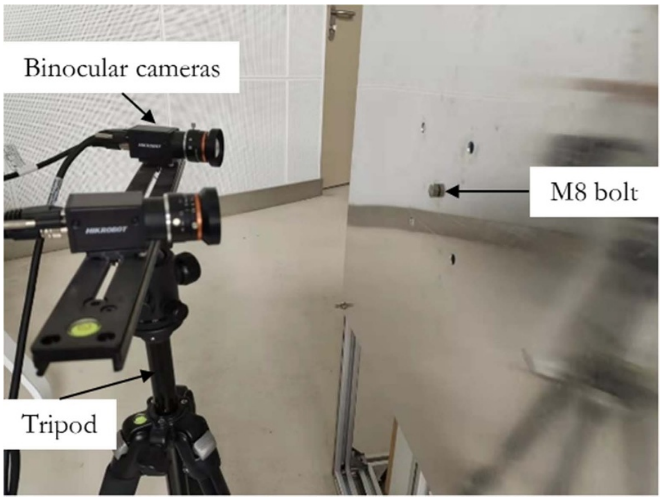

Figure 9. The experimental workbench.

Table 2. Detailed information of the cameras.

Model	MV-CA032-10GC
Image resolution	2048 × 1536
Sensor type	CMOS
Sensor size	1/1.8″
Data interface	Gige
Focal length	6 mm

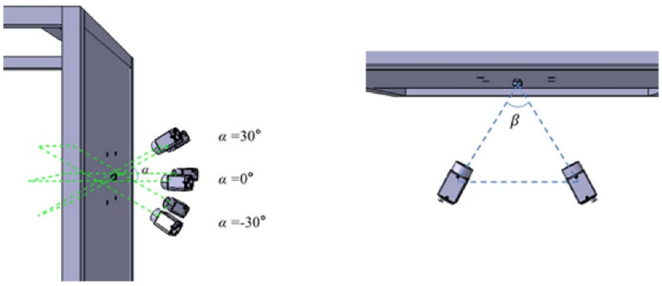

a. Vertical layout **b. Horizontal layout**

Figure 10. Layout of the binocular cameras.

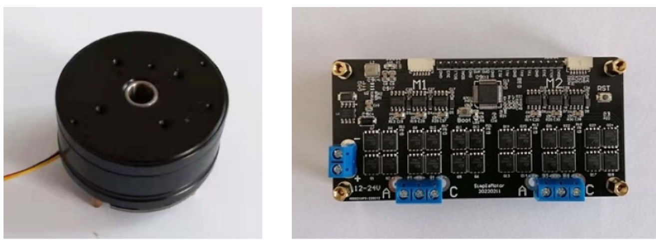

a.4108 motor with AS5600 encoder **b.SimpleMotor driveboard(based on STM32F103C8T6)**

Figure 11. The motor and the drive board.

3.2. Test on accuracy of the bolt loosening angle detection

In order to test the performance of the proposed method under various conditions, experiments are carried out using each key point detection models under the combinations of different

Figure 12. The experiment on actual bolt rotation angle measurement.

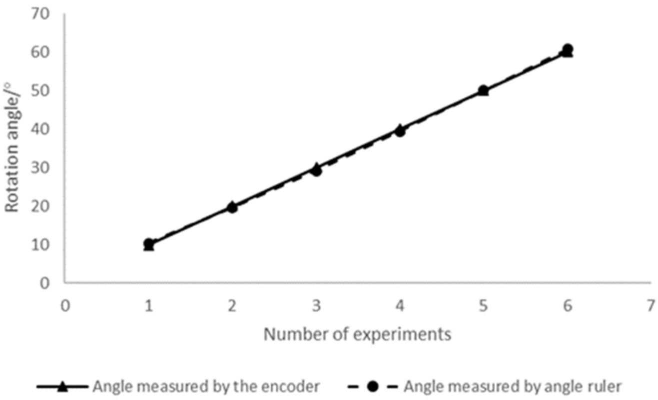

Figure 13. Angle measured by the encoder and angle ruler.

a. Exposure time = 60ms **b. Exposure time = 80ms** **c. Exposure time = 100ms**

Figure 14. Images captured under different exposure time.

vertical perspectives of camera (see figure 10(a)) and different exposure time. As shown in figure 14, different illumination conditions can be simulated by changing exposure time of the cameras. Under each condition, the servo motor is controlled to rotate the bolt to 0°, 5°, 10°, 20°, 30°, 40°, 50°, 60° in sequence. Images of the bolt at each rotated angle are captured by the binocular cameras simultaneously. Bolt rotated by 0° is considered as the intact state for reference and bolt at other rotation angles are considered as loosened, rotation angle is calculated by the proposed algorithm and compared with the encoder output angle. The experimental results are shown in figure 15.

Experimental results show that when the bolt rotation angle is in the range of [10°, 40°], all key point detection models can accurately track the real bolt loosening angle using least square fitting or RANSAC. As the rotation angle increased, the number of mismatches key point increased, and the accuracy of the least square algorithm decreased. When the bolt rotates 50°–60°, due to the rotation periodicity of the hexagon on the bolt surface, there are too many mismatches in the predictions of SPG-COCO-RGB and SPG-COCO-Gray (as shown in figure 16), and the RANSAC algorithm cannot correctly detect the bolt rotation angle due to the minority of inliers. SPG-Bolt-RGB using RANSAC algorithm can accurately track the rotation angle of the bolt with good robustness to illumination and perspective angle, with an average error of 1.5°. Angle measurement errors detected by SPG-Bolt-RGB using least square fitting or RANSAC under each condition presented in table 3 shows that RANSAC can effectively eliminate mismatches and reduce the error of detection results under the condition that correct predictions take the majority of total matches.

3.3. Detection of relative rotation between the bolt and the background

To verify the algorithm's capability to detect relative rotation between the bolt and the background, we run a test as follows. The background and the bolt are rotated at the same time, and the rotation angle of the background and the bolt are calculated by tracking the key points on the background image and the key points on the bolt surface, so as to calculate the relative motion between the bolt and the background. In the experiment, the bolt and the picture are not rotated for the intact state. For the loosened state, the background is rotated counterclockwise by 10°, 20° and 30° respectively, while the bolt is rotated clockwise by 10°, 20° and 30° for a total of nine groups of experiments are conducted. The SPG network model is retrained on the bolt images where a certain area around the bolt is reserved as background (named SPG-bolt-background-RGB), unlike pictures in the bolt imageset only contain bolt itself. The key point predictions made by SPG-bolt-background-RGB are compared with the models trained on the bolt images (SPG-bolt-RGB) and COCO (SPG-COCO-RGB), as shown in figure 17.

The average error of the bolt relative rotation angle measured by each key point detection model is shown in table 4. Results show that the measurement error of each key point detection model mainly comes from the measurement of the rotation angle of the background, because there are less distinguishing local features in the background, which makes it hard for machine learning and recognition. SPG-bolt-background-RGB outperforms the other two models in both bolt rotation angle detection and background detection, indicating that the key point detection model based on deep learning would perform better when the variance between the training set and the test set is small.

3.4. Comparison with monocular detection of bolt loosening angle

Related works that quantify the bolt loosening angle focus on HT-based monocular methods [16–22]. To verify the better

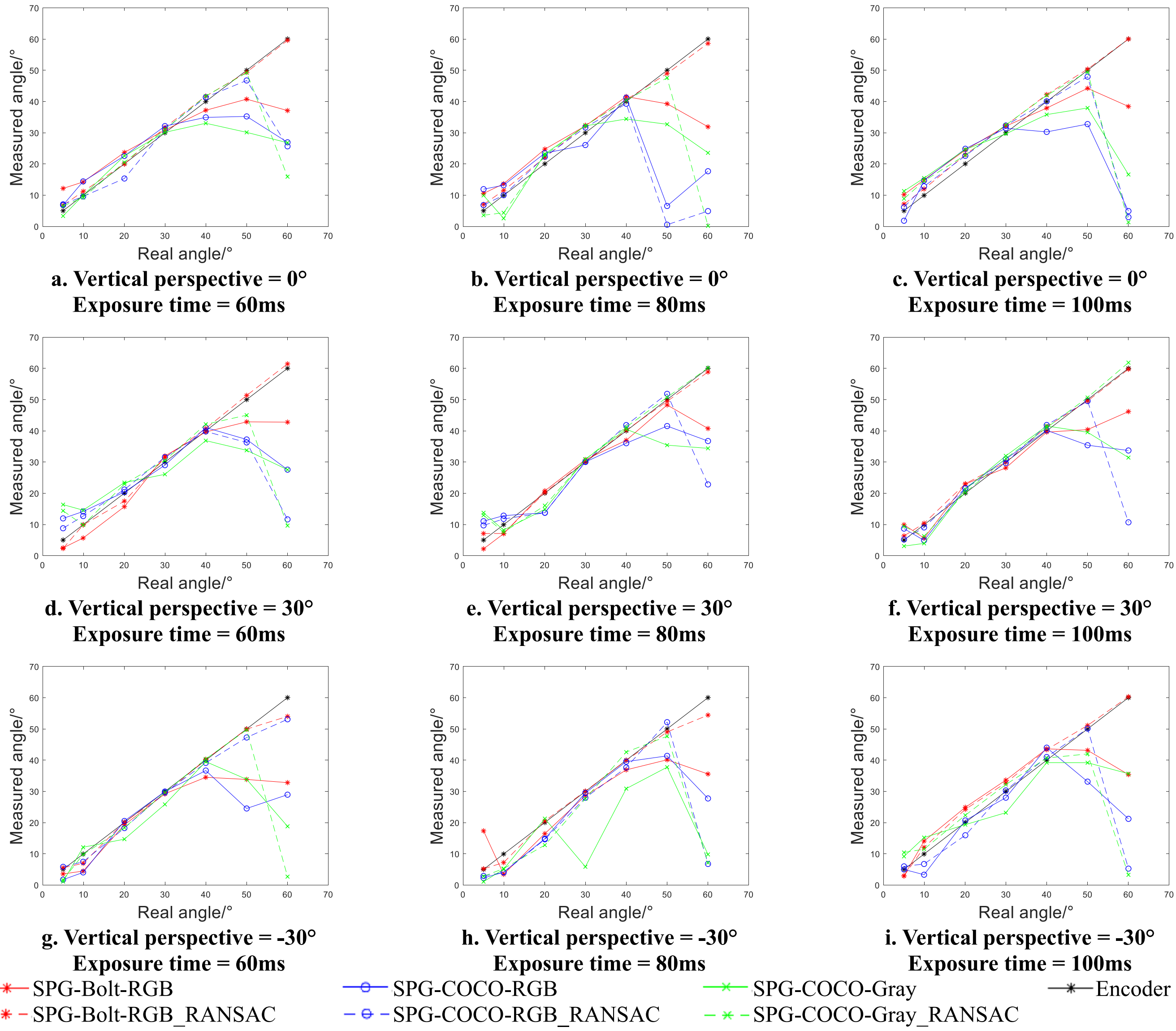

Figure 15. Experiment results under various conditions.

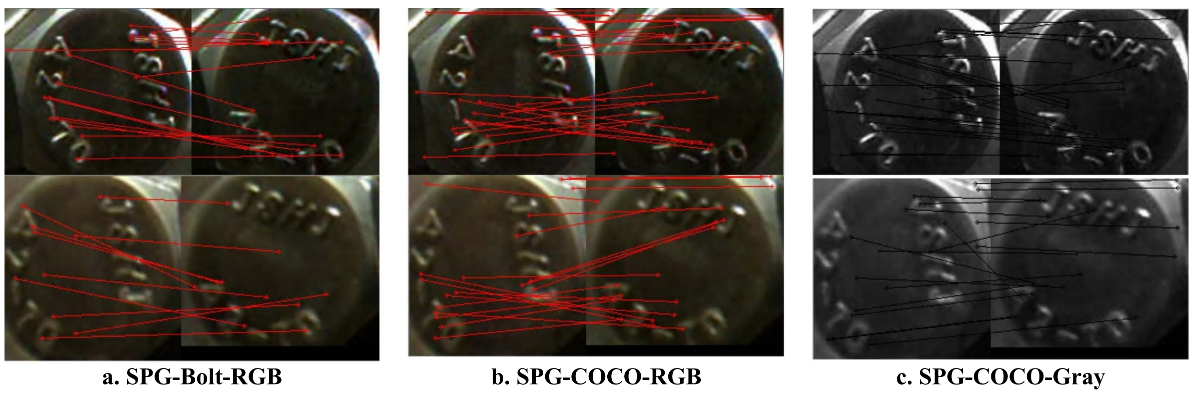

Figure 16. Key point match when the bolt rotates 60°.

performance of our binocular method under various conditions, bolt loosening angle detection based on monocular vision is tested using the same images captured in section 3.2 for the comparison. The specific implementation is as follows: after the bolt image is obtained through the object detection based on YOLO v4, the adaptive double threshold Canny edge

Table 3. The measurement error of SPG-bolt-RGB using least square fitting and RANSAC.

Vertical perspective	0°		30°		−30°	
Exposure time	Least square fitting	RANSAC	Least square fitting	RANSAC	Least square fitting	RANSAC
60 ms	7.3	1.1	5.4	1.4	5.4	1.5
80 ms	19.4	1.7	4.5	1.0	4.5	1.4
100 ms	6.6	1.7	5.4	1.0	5.4	2.3
Average error	11.1	1.5	5.1	1.2	5.1	1.8

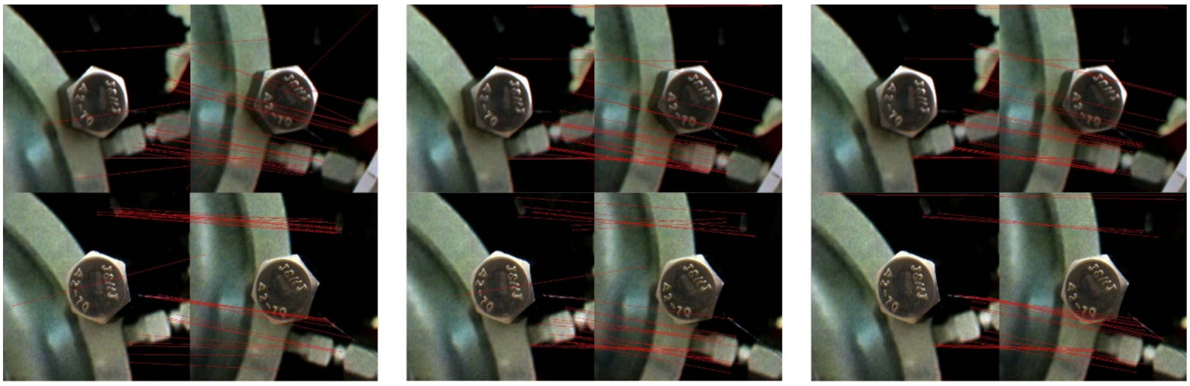

a. SPG-COCO-RGB b. SPG-Bolt-RGB c. SPG-Bolt-Background-RGB

Figure 17. Key point match on the background predicted by each SPG model.

Table 4. Average error of relative rotation angle detection.

Key point detection model	Error of rotation angle of the background	Error of rotation angle of the bolt	Error of relative rotation angle
SPG-COCO-RGB	5.3	1.8	6.8
SPG-bolt-RGB	3.8	1.3	4.4
SPG-bolt-background-RGB	2.8	1.2	2.8

detection is carried out on the bolt gray image as proposed in [20], then the edge is detected by HT, the score threshold of which is set to 0.2 times of the average of the length and width of the bolt image. Finally, the lines that constitute the hexagon of the bolt surface are filtered to exclude the false lines [17], among which the first three straight lines with the highest score are selected to calculate the angle. If no line is detected, 0° is returned as the current angle. Canny edge detection and HT line detection results are shown in figure 18. Due to the similar color between the background and the bolt surface and the interference of the pattern on bolt surface, sometimes there are too many false detections while sometimes there is no detected lines although the detection method is adaptive.

For the pictures taken by the left and right cameras in each experiment in section 3.2, the monocular detection of bolt loosening angle is carried out using the above method, the detection is tested and compared with the binocular method proposed in this paper as presented in figure 19. The results show that the accuracy of monocular method is equivalent to that of binocular method when the perspective angle is 0°. However, the monocular method is obviously affected by the distortion of image when there is a sharp perspective angle upward or downward with an average error more than 4° while that of binocular method is only 1.5°. The experiment illustrates that it is difficult for the monocular method to eliminate the error caused by the perspective angle without the bolt position information as reference for distortion correction of the image, while the binocular method is robust to the camera perspective angle by restoring the three-dimensional information of the key points. Therefore the proposed bolt loosening angle detection method based on binocular vision has less limitations and better applicability compared to previous method based on monocular vision.

4. Discussion

To further investigate the relationship between the performance of the proposed algorithm and cameras' pose, bolt loosening angle measurement are tested under different α and β (defined in figure 10). Experimental results are shown in figures 20 and 21.

The proposed method presents high measurement accuracy when $\alpha < 50°$ and $\beta < 70°$. When the horizontal or vertical angle of cameras goes sharper, the method produces poorer

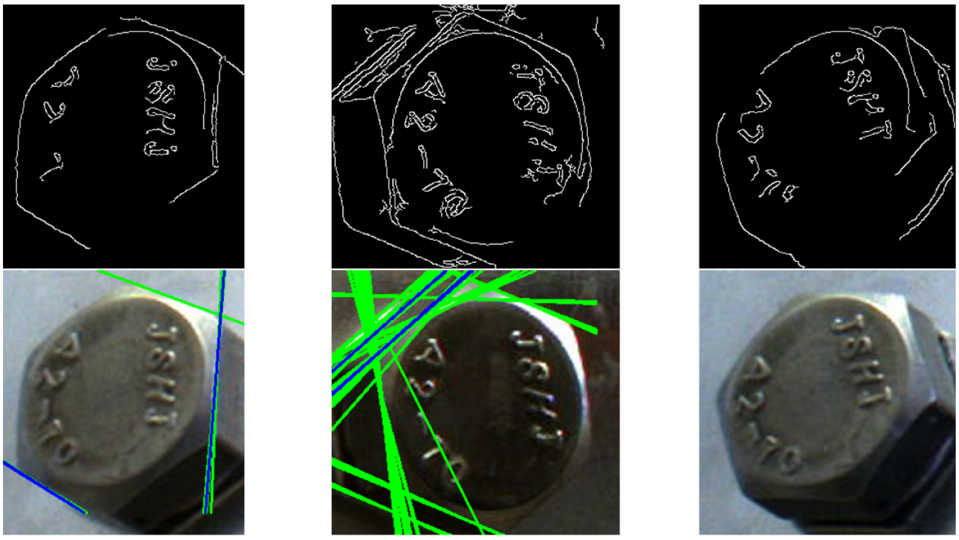

a. Correct detections b. Too many false detections c. No line detected

Figure 18. Canny edge detection and HT line detection (blue for detected lines, green for selected lines).

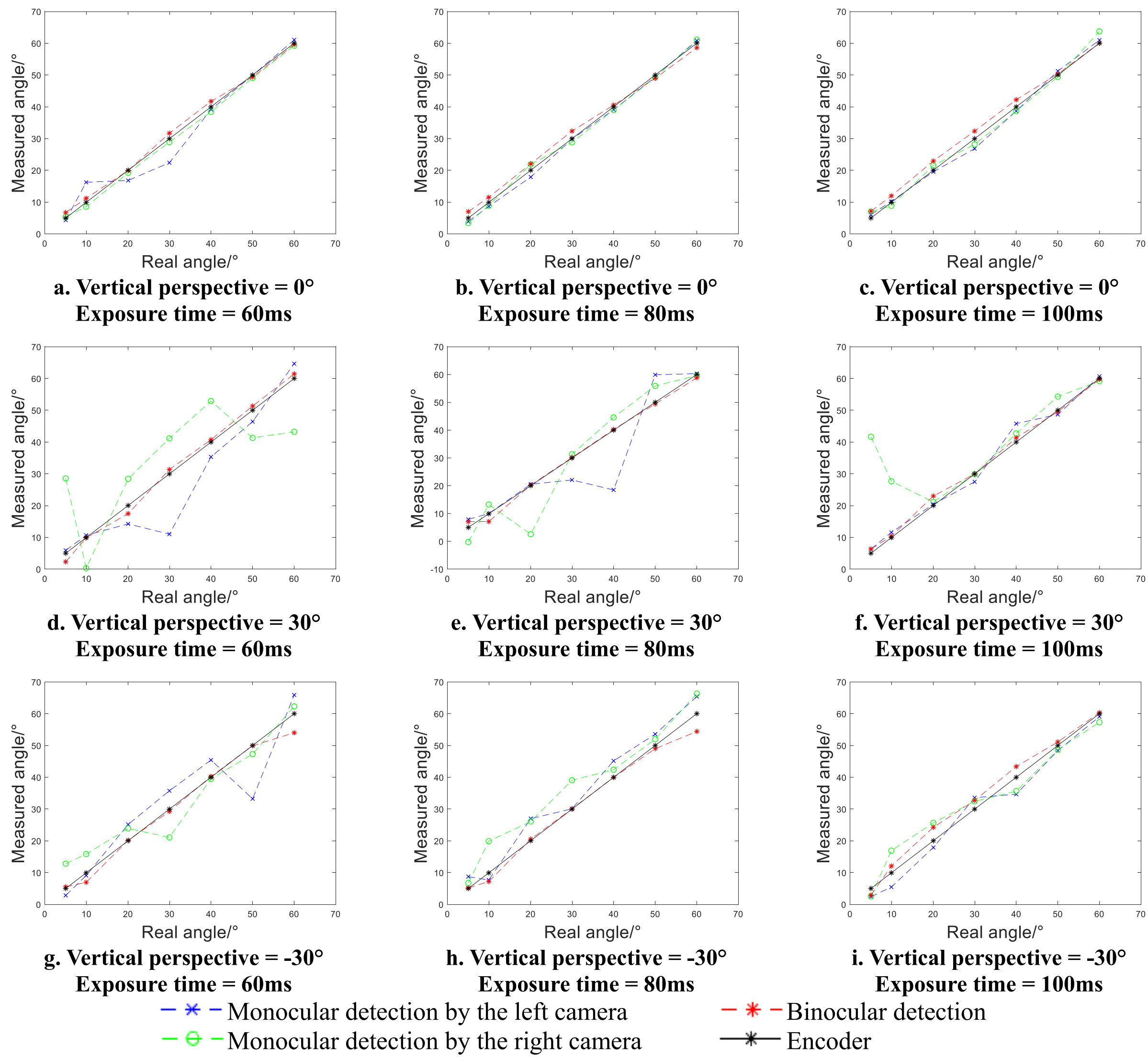

Figure 19. Comparison of bolt loosening angle detection based on monocular vision and binocular vision.

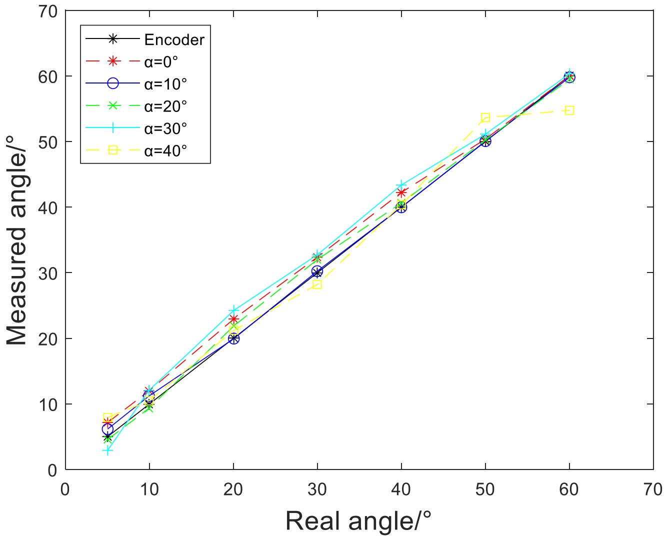

Figure 20. Measurement results under different vertical angle of cameras α (with β fixed at 20°).

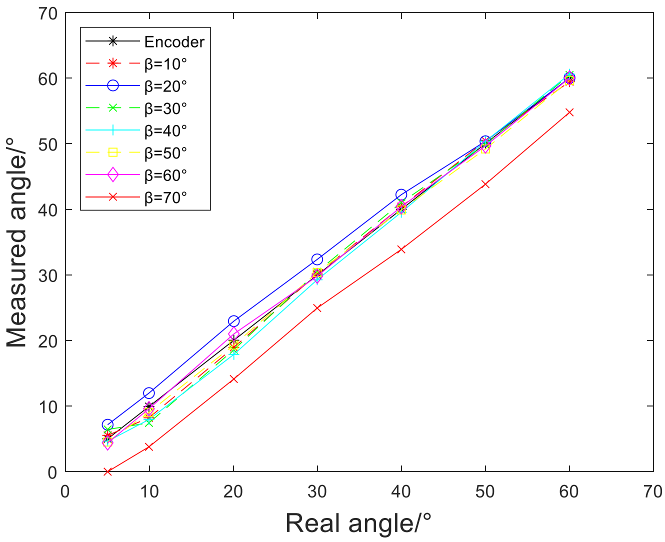

Figure 21. Measurement results under different vertical angle of cameras β (with α fixed at 0°).

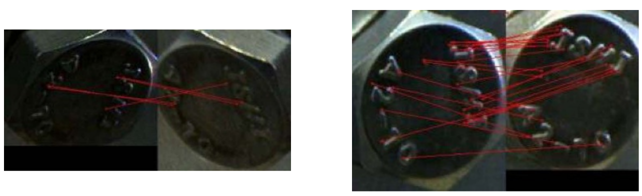

a. Sparse stereo matches that lead to 3D reconstruction failure when *α*=50°

b. Incorrect motion matches that lead to accuracy loss when *β*=70°

Figure 22. Matches produced under sharp vertical or horizontal angle of cameras.

result or malfunctions due to the scanty correct matches as a result of less sematic information obtained by the cameras (see figure 22). Therefore, it is suggested the proposed method is implemented under cameras' horizontal angle $\alpha < 50°$ and vertical angle $\beta < 70°$.

5. Conclusion

In this study, we propose a novel binocular vision-based method for detecting the angle loosening angle. Key points on the bolt are detected and matched for three-dimensional reconstruction and motion tracking, and the rotation angle is solved by the rotation equation using RANSAC. Experiments verifies that the feasibility and superiority of the proposed method in following aspects:

(a) The proposed method is robust to illumination condition and the vertical perspective of camera with an average error of 1.5°. The key point detector trained on the bolt images has higher accuracy than that trained on COCO as the benefit of transfer learning.
(b) The monocular vision-based method is tested under the same conditions for comparison, and the result shows that the binocular vision-based method is invariant to the error caused by perspective distortion that affects the accuracy of monocular vision-based method to a great extent.
(c) Relative rotation detection is also tested to stimulate relative motion between the cameras and the background. The key point detector trained on bolt images with background can predict more accurate matches on both bolt and background, and the relative angle can be detected correctly with an average error of 2.8°. It indicates that the proposed key point-based bolt looseness detection is capable of eliminating the relative motion between the cameras and the background.

To sum up, the proposed method presents robustness to different conditions and superiority to previous monocular vision-based detection. Under cameras' horizontal angle $\alpha < 50°$ and vertical angle $\beta < 70°$, and our algorithm produces accurate quantified bolt loosening angle at early stage without extra marks or specific requirements of bolts arrangement. Our method focuses on detecting small bolt loosening angle θ with an average error of 1.5° when $\theta \in [0°, 60°]$, while larger looseness can be identified by detecting the exposed length of the screw. In addition, the key point tracking-based detection shows its potential in the field of motion measurement and is worth of further research in the future.

Data availability statement

All data that support the findings of this study are included within the article (and any supplementary files).

ORCID iDs

Shixu Wang https://orcid.org/0000-0001-5797-7750
Jiang Wu https://orcid.org/0000-0003-2888-6520

References

[1] Wang T, Song G, Liu S, Li Y and Xiao H 2013 Review of bolted connection monitoring *Int. J. Distrib. Sens. Netw.* **9** 871213

[2] Zhang J 2017 Condition monitoring and typical fault diagnosis of aero-engine Shenyang Aerospace University

[3] Wang F, Ho S C M and Song G 2019 Monitoring of early looseness of multi-bolt connection: a new entropy-based active sensing method without saturation *Smart Mater. Struct.* **28** 964–1726

[4] Kim N and Hong M 2009 Measurement of axial stress using mode converted ultrasound *NDT&E Int.* **42** 164–9

[5] Shao J, Wang T, Yin H, Yang D and Li Y 2016 Bolt looseness detection based on piezoelectric impedance frequency shift *Appl. Sci.* **6** 298

[6] Sun W and Zhang Y 2013 Numerical simulation of bolt looseness monitoring based on impedance method *Appl. Mech. Mater.* **351–352** 1264–8

[7] Wang F Song G2021 A novel percussion-based method for multi-bolt looseness detection using one-dimensional memory augmented convolutional long short-term memory networks *Mech. Syst. Signal Process.* **161** 107955

[8] Na W S 2021 Bolt loosening detection using impedance based non-destructive method and probabilistic neural network technique with minimal training data *Eng. Struct.* **226** 111228

[9] Li Z-J, Adamu K, Yan K, Xu X-L, Shao P, Li X-H and Bashir H M 2022 Detection of nut–bolt loss in steel bridges using deep learning techniques *Sustainability* **14** 10837

[10] Cha Y-J, You K and Choi W 2016 Vision-based detection of loosened bolts using the Hough transform and support vector machines *Autom. Constr.* **71** 181–8

[11] Ramana L, Choi W and Cha Y J 2019 Fully automated vision-based loosened bolt detection using the Viola-Jones algorithm *Struct. Health Monit.* **18** 422–34

[12] Zhang Y, Sun X, Loh K J, Su W, Xue Z and Zhao X 2020 Autonomous bolt loosening detection using deep learning *Struct. Health Monit.* **19** 105–22

[13] Sun J, Xie Y and Cheng X 2020 A fast bolt-loosening detection method of running train's key components based on binocular vision *IEEE Access* **7** 32227–39

[14] Jiang Y, Zhang M and Lee C-H 2003 A study of early stage self-loosening of bolted joints *ASME J. Mech. Des.* **125** 518–25

[15] Kong X and Li J 2018 Image registration-based bolt loosening detection of steel joints *Sensors* **18** 1000

[16] Nguyen T C, Huynh T C, Ryu J Y, Park J H and Kim J T 2016 Bolt-loosening identification of bolt connections by vision image-based techniqueBolt-loosening identification of bolt connections by vision image-based technique *Proc. SPIE* **9804** 980413

[17] Liao R 2019 Anomaly object detection based on deep learning Southeast UniversitySoutheast University

[18] Huynh T-C, Park J-H, Jung H-J and Kim J-T 2019 Quasi-autonomous bolt-loosening detection method using vision-based deep learning and image processing *Autom. Constr.* **105** 102844

[19] Quoc-Bao T and Kim J T 2020 Monitoring of corroded and loosened bolts in steel structures via deep learning and Hough transforms *Sensors* **20** 6888

[20] Huynh T-C 2021 Vision-based autonomous bolt-looseness detection method for splice connections: design, lab-scale evaluation, and field application *Autom. Constr.* **124** 103591

[21] Pham H C, Quoc-Bao T, Kim J-T, Duc-Duy H, Tran X-L and Huynh T-C 2020 Bolt-loosening monitoring framework using an image-based deep learning and graphical model *Sensors* **20** 3382

[22] Wang C, Wang N, Siu-Chun H, Chen X and Song G 2020 Design of a new vision-based method for the bolts looseness detection in flange connections *Sensors* **67** 2

[23] Zhao X, Zhang Y and Wang N 2019 Bolt loosening angle detection technology using deep learning *Struct. Control. Health Monit.* **26** 2292

[24] Yu Y, Liu Y, Chen J, Jiang D, Zhuang Z and Wu X 2021 Detection method for bolted connection looseness at small angles of timber structures based on deep learning *Sensors* **21** 3106

[25] Yang X, Gao Y, Fang C, Zheng Y and Wang W 2022 Deep learning-based bolt loosening detection for wind turbine towers *Struct. Control. Health Monit.* **29** e2943

[26] Cui H, Qingwu H and Mao Q 2018 Real-time geometric parameter measurement of high-speed railway fastener based on point cloud from structured light sensors *Sensors* **18** 3675

[27] Mao Q, Cui H, Hu Q and Ren X 2018 A rigorous fastener inspection approach for high-speed railway from structured light sensors *ISPRS J. Photogramm. Remote Sens.* **143** 249–67

[28] Lorente A, Llorca D, Velasco M, García J and Domínguez F 2014 Detection of range-based rail gage and missing rail fasteners: use of high-resolution two-and three-dimensional images *Transp. Res. Rec. J. Transp. Res. Board* **2448** 125–32

[29] Bochkovskiy A, Wang C-Y and Liao H-Y M 2020 YOLOv4: optimal speed and accuracy of object detection (arXiv:2004.10934)

[30] Lowe D G 2004 Distinctive image features from scale-invariant keypoints *Int. J. Comput. Vis.* **60** 91–110

[31] Detone D, Malisiewicz T and Rabinovich A 2018 SuperPoint: self-supervised interest point detection and description *IEEE/CVF Conf. on Computer Vision and Pattern Recognition Workshops (CVPRW)* vol 12 p 337

[32] Jau Y-Y, Zhu R, Hao S and Chandraker M 2020 Deep keypoint-based camera pose estimation with geometric constraints *IIEEE/RSJ nt. Conf. on Intelligent Robots and Systems (IROS)* pp 4950–7

[33] Simonyan K and Zisserman A 2014 Very deep convolutional networks for large-scale image recognition (arXiv:1409.1556)

[34] Lin T-Y, Maire M, Belongie S, Hays J, Perona P, Ramanan D, Doll´ar P and Zitnick L 2014 Microsoft COCO: common objects in context *European Conf. on Computer Vision (ECCV)* pp 740–55

[35] Balntas V, Lenc K, Vedaldi A and Mikolajczyk K 2017 HPatches: a benchmark and evaluation of handcrafted and learned local descriptors *Conf. on Computer Vision and Pattern Recognition (CVPR)* pp 5173–82

[36] Zhang Z 2000 A flexible new technique for camera calibration *IEEE Trans. Pattern Anal. Mach. Intell.* **22** 11

[37] Faugeras O D 1992 What can be seen in three dimensions with an uncalibrated stereo rig? *European Conf. on Computer Vision (ECCV)* pp 563–78

[38] Fischler M A and Bolles R C 1981 Random sample consensus: a paradigm for model fitting with applications to image analysis and automated cartography *Commun. ACM* **24** 381–95